VELOCITY PROFILES OF FLUID/PARTICULATE MIXTURES IN PIPE FLOW USING MRI

KATHRYN L. McCARTHY[1], WILLIAM L. KERR, ROBERT J. KAUTEN and JEFFREY H. WALTON[2]

Department of Food Science and Technology
[2]UCD NMR Facility
University of California
Davis, CA USA 95616

Accepted for Publication August 15, 1996

ABSTRACT

Magnetic resonance imaging (MRI) techniques have been utilized to experimentally measure velocity profiles and apparent rheological properties of fluid/particulate mixtures as functions of flow rate, particle loading, and particle size. The experimental velocity profiles were described by a power law model for these systems. A 3% aqueous sodium alginic acid solution was used to form two particle sizes of 2.5 mm and 5.0 mm in diameter. The spheres were suspended in a 0.5% carboxymethyl cellulose solution at loadings of 0, 10, 20, and 30% by weight. The average fluid velocity ranged from 2-35 cm/s. The flow behavior index decreased as flow rate, particle loading or particles size increase. Cumulative residence time curves were evaluated based on this modeling procedure. Results of this research have direct application to aseptic processing of fluid/particulate mixtures.

INTRODUCTION

Aseptic processing and filling consists of presterilizing a food product before filling a sterile package. The atmosphere and mechanical means of closing the package must also be sterile. This type of processing has several advantages, primarily in the quality of the treated foods and ease or cost of storage and distribution. However, limitations to aseptic processing still exist in the area of presterilization of difficult products, such as liquids with large particles (Buchner 1993). The heat sterilization of fluid/particulate mixtures requires that the products are heated to an appropriately high temperature and maintained at that temperature for a given period in order to achieve the desired

[1] To whom correspondence should be addressed. Tel: 916-752-1487, FAX: 916-752-4759

Journal of Food Process Engineering **20** (1997) 165-177. *All Rights Reserved.*

degree of sterility. The time/temperature process must ensure that the fastest moving particles in the continuous system receive adequate heat treatment. In many cases, the heat treatment of these fluid/particulate mixtures incorporates tube-type heat exchangers and holding tubes. However, the lack of fundamental information on particle and fluid flow in holding tubes has to date limited the application of this technology (Sastry 1989). This lack of fundamental knowledge results in over processing and substantial product degradation.

The objectives of this study were to measure velocity profiles and apparent rheological properties of fluid/particulate mixtures under conditions relevant to aseptic processing. Current techniques include dye tracer (Singh and Lee 1992), timed collection (Hong *et al.* 1991), Hall effect (Tucker and Withers 1994), photo sensor (Yang and Swartzel 1992), video image analysis (Simunovic *et al.* 1995), hot wire anemometry, and Doppler ultrasonic methods (Fregert and Tragardh 1995). Developments in nuclear magnetic resonance (NMR) and imaging capabilities have allowed magnetic resonance imaging (MRI) techniques to be used for flow measurements. One advantage to MRI is that it is noninvasive and does not require the addition of special particles to the flow medium. In addition, any given slice of fluid can be sampled and velocity profiles developed for that slice. MRI velocity phase encode techniques are well covered in the literature (Stepisnik 1985; Caprihan and Fukushima 1990; Callaghan 1991; Pope and Yao 1993). The velocity phase encode technique utilized in this work is a spin echo method (Hahn 1950; Carr and Purcell 1954) using pulsed magnetic field gradients (Stejskal 1965) which measures the displacement probability of an ensemble of nuclei localized within a voxel of the sample flowing through a pipe.

THEORY

In order to characterize the rheological behavior or apparent rheological behavior, a power law model was used to model the velocity profiles of the fluid and fluid/particulate mixtures. For this approach, the relationship between the velocity, v, at the radial position r and the volumetric average velocity, $<v>$, is

$$\frac{v}{<v>} = \left[\frac{3n+1}{n+1}\right]\left[1-\left[\frac{r}{R}\right]^{(n+1)/n}\right] \tag{1}$$

where R is the inner radius of the pipe (Steffe 1992). This expression arises from integration of the force balance for pipe flow with the incorporation of

$$\sigma = K\dot{\gamma}^n \tag{2}$$

to describe the relationship between shear stress, σ, and shear rate, $\dot{\gamma}$, where K is the consistency coefficient and n is the flow behavior index. $\dot{\gamma}$ is the derivative of v with respect to radial position. In this study, n is a true rheological parameter for only the homogeneous CMC solutions (no particles) in steady laminar flow. However, the flow behavior index allows us to describe the apparent rheological behavior of the fluid/particulate mixtures under the specified flow condition. In other words, n characterizes the degree of "bluntness" of the velocity profile. This approach to modeling allows a straightforward comparison of velocity profiles and residence time distributions (RTD) as a function of flow rate, particle loading, and particle size.

The residence time distribution, which is a standard technique to describe the uniformity of the history of the material in the system, is a function of the flow behavior index. Middleman (1977) outlined the procedure to evaluate the residence time of a Newtonian fluid in laminar flow in a pipe from the velocity profile. The following analysis is for power law fluids and incorporates the velocity profile for these fluids given in Eq. (1). Consider an element of fluid at radial position r. The element moves at velocity $v(r)$ through an axial distance L in the time given by

$$t = \frac{L}{v(r)} \tag{3}$$

Fluid elements which all enter the pipe at the same time will leave at different times as a function of their radial position. For a quantitative interpretation of residence time, the function $f(t)$ is defined such that $f(t)\,dt$ is the fraction of the output of the flow which had been in the pipe for a time in the range t to $t+dt$.

$$f(t)dt = \frac{d\dot{V}}{\dot{V}} = \frac{2\pi r v(r) dr}{\pi R^2 \langle v \rangle} = \frac{2r}{R^2} \frac{v(r)}{\langle v \rangle} dr \tag{4}$$

where $d\dot{V}$ is the incremental change in volumetric flow rate, $\dot{V}$. The cumulative residence time distribution function, or F function, is an integration of Eq. (4),

$$F(t) = \int_{t_o}^{t} f(t)dt \tag{5}$$

where the lower limit is the first appearance time and corresponds to the fluid moving along the pipe axis ($r = 0$) where the velocity is the greatest. Therefore in terms of velocity, the cumulative residence time distribution for a power law fluid is

$$F(t)=\int_{t_o}^{t}\frac{d\dot{V}}{\dot{V}}=\int_{r=0}^{r}\frac{2r}{R^2}\left(\frac{3n+1}{n+1}\right)\left[1-\left(\frac{r}{R}\right)^{(n+1)/n}\right]dr \qquad (6)$$

The ideal residence time is a unit step function, which would correspond to plug flow. This condition is "ideal" since all fluid elements have exactly the same residence time in the pipe. Because of no-slip condition at the pipe wall, the plug flow condition can only be approached.

MATERIALS AND METHODS

The flow loop was constructed of 26.2 mm i.d. clear PVC pipe. A straight length of pipe with a length of 175 pipe diameters preceded the section centered in the horizontal bore of the 2 T Oxford magnet. The magnet was connected to a General Electric CSI-II NMR imaging spectrometer operating at a proton frequency of 85.5 MHz. The receiver/transmitter for the radio frequency signal was a 100 mm bird-cage coil. A positive displacement pump (SPS-20, Sine Pump, Orange, MA) circulated the fluid and fluid/particulate mixtures through the flow loop.

The model particulates were 2.5 and 5.0 mm diameter gel spheres. These spheres were formed with an aqueous 3 wt. % sodium alginic acid (Sigma Chemical, St. Louis, MO). The alginic acid solution was prepared and agitated for 8 h. The aqueous solution was then pumped via a syringe pump into a 0.08 M (minimum) calcium chloride solution for gelation, with calcium acting as a crosslinking agent. Two different syringes were used to form the spheres; the syringe size determined the relative contribution of gravity and surface tension and therefore, the drop size. Once formed, the alginate drops were allowed to gel completely in the calcium chloride solution over an 8 h period. The solution was stirred to prevent deformation of the spheres upon settling.

The suspending fluid was a 0.5 wt % carboxymethyl cellulose (CMC) (Methocel, Dow Chemical Co., Midland, MI) solution. The fluid had a density of 1.01 g/mL and consisted of 66 g of CMC, 500 mL of methanol (0.79 sp gr), and 13 L of deionized water. The purpose of the methanol was to solubilize the CMC prior to hydration. The CMC solution was best characterized as a power law fluid; the flow behavior index, n, was determined by the best power law fit of the velocity profile (Eq. 1) with regression coefficients greater than or equal to 0.998 in all cases. These flow behavior indices were a function of flow rate and varied slightly between batches of CMC solution. The three batches of CMC solution used in this study have been characterized in Table 1. The shear rate ranges were determined by differentiation of the fits to Eq. 1.

TABLE 1.
CHARACTERIZATION OF THREE BATCHES OF CMC SOLUTION USED AS SUSPENDING FLUID

Batch	n	Ave. Velocity (cm/s)	Shear Rate Range (s^{-1})	R
1	0.72	34.6	0 - 60	0.999
	0.85	15.3	0 - 35	0.999
	0.83	7.4	0 - 15	0.999
	0.94	2.2	0 - 6	0.999
2	0.88	16.1	0 - 40	0.999
3	0.95	17.2	0 - 50	0.998

For the fluid/particulate suspensions, the gel spheres were suspended in the CMC solution at loadings of 10, 20, and 30% by weight. Imaging experiments were performed in the flow rate range from 12 to 186 cm^3/s.

NMR Method

The NMR flow imaging technique yields a joint spatial-velocity ^1H spin density distribution. The NMR pulse sequence consists of three basic parts — slice selection, velocity encoding, and frequency encoding — to provide the axial velocity versus radial position within the pipe. Since, the flow was along the magnet axis in the z direction, the slice selection was done with the z gradient. The resulting slice was a 2 mm thick disk across the pipe. Velocity encoding with the z gradient then tags the z component of the velocity. Finally, frequency encoding in the x direction reads out the radial position of the volume elements. There were 128 phase encode steps and 128 points were used to digitize each echo. The resulting matrix was zero filled to 256 × 256 and a 2D fourier transform performed. The plot of velocity versus radial position was determined by the maximum signal intensity in each row of the matrix. The velocity profile was fit to power law model using commercially available nonlinear least squares fitting routine (KaleidaGraph, Abelbeck Software).

RESULTS AND DISCUSSION

Figure 1 illustrates an example of a joint spatial-velocity ^1H spin density distribution images for the pure suspending fluid and a fluid/particulate mixture. The signal intensity portrays the axial velocity as a function of radial position, with the maximum velocity at the centerline and a no-slip condition at the pipe wall. In Fig. 1(a) the signal intensity of the pure fluid is uniform and has the characteristic blunting of a pseudoplastic (i.e., shear thinning) fluid. The average

(a)

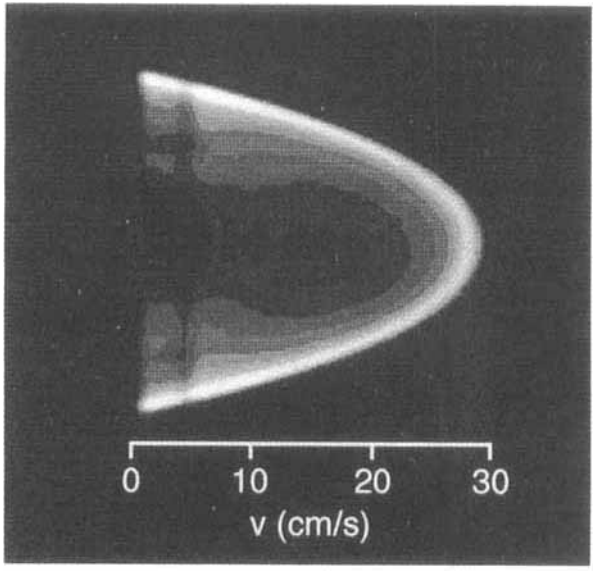

(b)

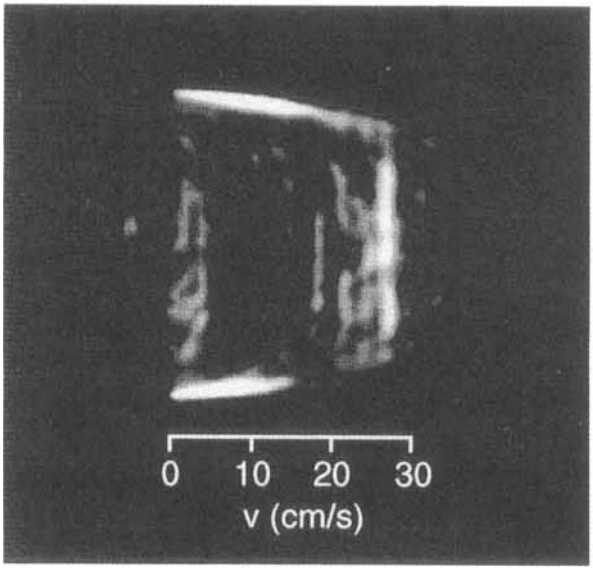

FIG. 1. REPRESENTATIVE MR FLOW IMAGES FOR THE (a) PURE SUSPENDING FLUID AND (b) A FLUID/PARTICULATE MIXTURE AT A 20% LOADING OF 2.5 MM DIAMETER GEL SPHERES

velocity of the fluid was 15.3 cm/s with a maximum velocity of 29.4 cm/s; the flow behavior index of the fluid under these conditions was 0.85. Figure 1(b) illustrates the image obtained at 20% particle loading of the 2.5 mm diameter spheres at an average velocity of 18.1 cm/s. This image illustrates a greater degree of blunting as compared to the pure suspending fluid and has been characterized by an n of 0.41.

Flow Profiles as a Function of Flow Rate

Velocity profiles of the pure suspending fluid were obtained at several flow rates from 12 to 186 cm^3/s, which correspond to average velocities of 2.2 to 34.6 cm/s, respectively. As shown in Table 1, the flow behavior index of Batch 1 of 0.5% CMC solution is a function of shear rate range, i.e., flow rate. As expected for a power law fluid, the profiles become more blunt as the flow rate increases. As the flow rate increased the flow behavior index decreases from 0.94 to 0.72. This blunting results in a maximum velocity that is closer to the average velocity and more uniform treatment of the fluid. This change in rheological parameter would not occur if the suspending fluid had been a Newtonian fluid. Therefore, when evaluating the profiles of fluid/particulate mixtures, there is a contribution to the blunting from both the pure fluid as well as the suspended particles. To illustrate this concept, Fig. 2 plots the velocity

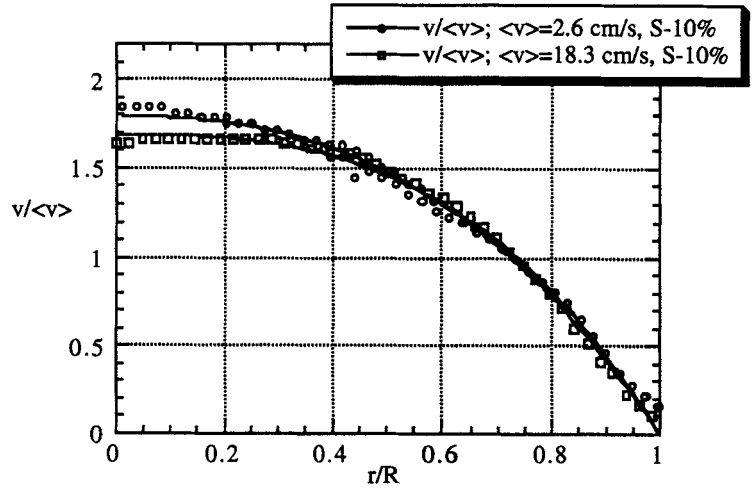

FIG. 2. AS WITH PURE FLUID, FLOW PROFILES FOR THE FLUID/PARTICULATE MIXTURES ARE A FUNCTION OF FLOW RATE

Here, a mixture of 10% loading of small spheres are shown at a fluid/particulate velocity of 2.6 cm/s and 18.3 cm/s shown with the power law fit of the experimental data. The suspending fluid is the same batch of CMC solution.

profiles for a fluid/particulate mixture at 10% loading of 2.5 mm diameter gelspheres. The velocity profiles are dimensionless by the average velocity of the flowing fluid, $<v>$ and the pipe radius, R. The average velocity of the upper curve is 2.6 cm/s and that of the lower curve is 18.3 cm/s. Not only are the flow indices considerably lower than that of pure fluid (Table 2), but the change in n is greater than that of pure fluid for comparable flow rates. In other words, the ratio of n values of the lower flow rate to higher flow rate is 1.25 for the fluid/particulate mixture and 1.11 for the pure suspending fluid.

TABLE 2.
CHARACTERIZATION OF FLUID/PARTICULATE MIXTURES

Particle Loading	Suspending Fluid Batch	n	Ave. Velocity (cm/s)	R
Small				
10	1	0.65	2.6	0.996
20	1	0.41	18.1	0.999
30	2	0.33	21.1	0.996
Large				
20	3	0.20	17.5	0.988

Flow Profiles as a Function of Particle Loading

Figure 3 illustrates the change in the shape of the velocity profiles for fluid/particulate mixtures as a function of particle loading. The 2.5 mm diameter particles are shown at loadings of 0, 10, 20% in Fig. 3(a) and 0% and 30% loading in Fig. 3(b); the suspending fluid (i.e., 0% loading) in these two figures is different (see Table 2). These profiles are obtained at an average velocity in the range of 18 $\pm$ 3 cm/s, thereby minimizing the contribution of the flow rate differences in the comparisons. The addition of particles is a significant contribution to the change in the flow behavior index. The value of n drops from 0.85 to 0.65 with a 10% loading of 2.5 mm diameter particles. As the particle loading increases to 30%, the flow index drops to 0.33. This decrease in flow behavior index from 0.85 to 0.33 changes the ratio of maximum velocity to average velocity from 1.92 to 1.50. The practical implication is that holding tubes designed assuming a maximum velocity that is twice the average velocity (i.e., Newtonian fluid) over processes fluid/particulate mixtures.

Flow Profiles as a Function of Particle Size

Velocity profiles of the fluid/particulate mixtures are also a function of particle size. Figure 4 illustrates the extent of blunting at 20% loading for small

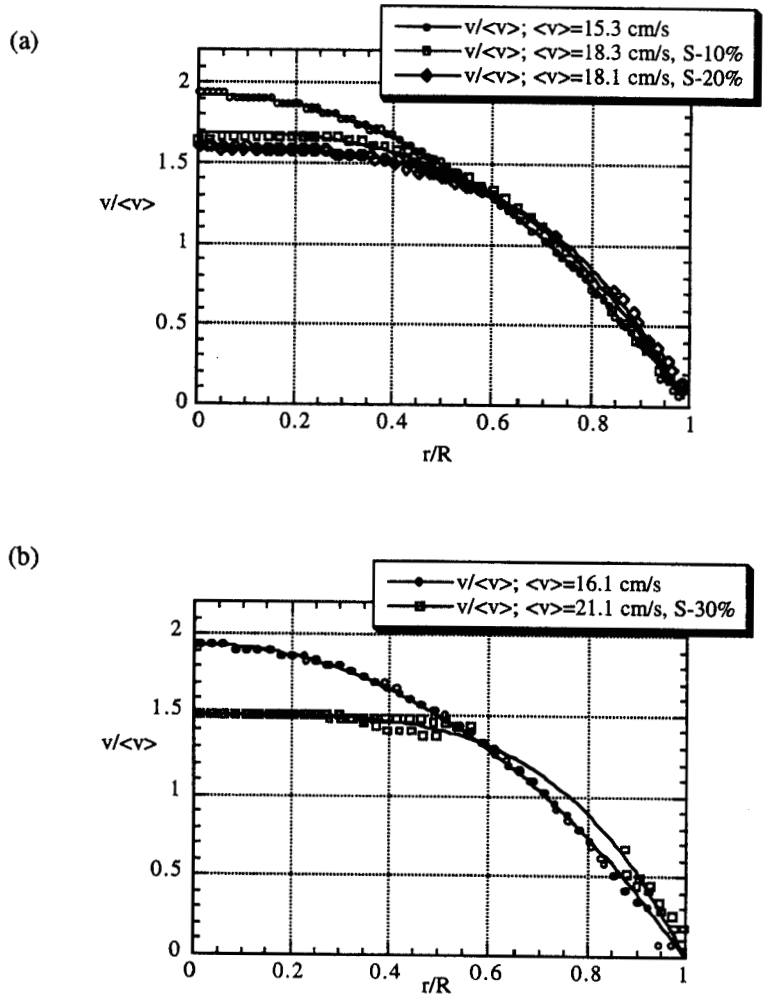

FIG. 3. VELOCITY PROFILES FOR FLUID/PARTICULATE MIXTURES AT PARTICLE LOADINGS OF (a) 10% AND 20%, AND (b) 30%
For each fluid/particulate mixture, the velocity profile for the pure suspending fluid is also shown at approximately the same volumetric flow rate with its power law fit.

particles (2.5 mm diameter) and large particles (5.0 mm diameter). The fluid/particulate mixtures shown in Fig.4 (a) and 4(b) are compared to their own suspending fluid at average velocities in the range of 16.7 $\pm$ 1.4 cm/s. Under these conditions, the ratio of $n/n_{suspending}$ is 0.48 and 0.21 for small and large particles, respectively.

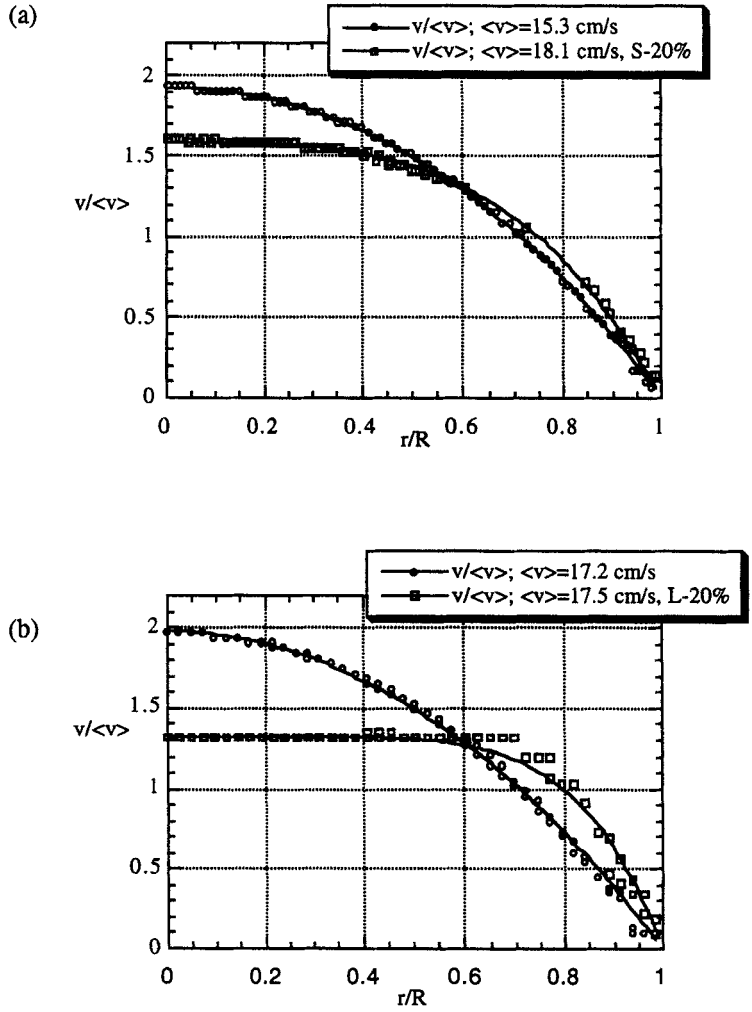

FIG. 4. THE EXTENT OF BLUNTING OF THE VELOCITY PROFILE IS ALSO A FUNCTION OF PARTICLE SIZE AS SHOWN AT 20% LOADING WITH SMALL PARTICLES IN (a) AND LARGE PARTICLES IN (b)
Each of the fluid/particulate mixtures is referenced to its own suspending fluid; the curves are the power law fit of the experimental data.

Residence Time Distribution Curves

The residence time distribution curve is altered considerably as the velocity profile becomes blunter. Figure 5 illustrates the *F(t)* curve for the flow behavior

indices that characterize the velocity profiles given in Fig. 4. The vertical line at $t/<t> = 1.0$ is the curve for plug flow, where $<t>$ is the average time; all fluid has traveled through the pipe with the same uniform history. The other limiting case is the curve for a Newtonian fluid ($n = 1$) which yields the greatest deviation of the cases shown with respect to the history of the fluid elements. The first appearance time, which is the shortest time fluid resides in the pipe is $t/<t> = 0.5$. Under these flow conditions, at $5<t>$, 1% of the fluid still resides in the pipe. By contrast, as n decreases, the first appearance time approaches $t/<t> = 1.0$.

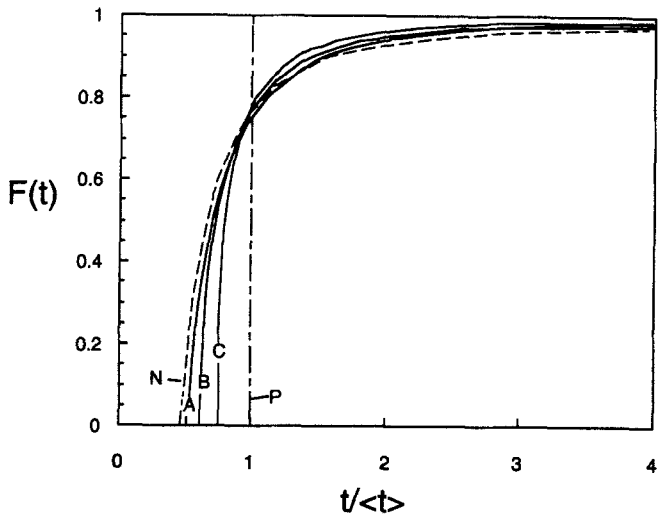

FIG. 5. RTD FOR PLUG (P) FLOW, AND FOR FLUIDS WITH FLOW BEHAVIOR INDICES OF 1.0 (N), 0.85 (A), 0.41 (B), AND 0.20 (C)

Also shown are RTD curves for the following systems: 0.5% CMC, $<v> = 15.3$ cm/s, n=0.85; 20% particles (2.5 mm), $<v> = 18.1$ cm/s, n=0.41; and 20% particles (5.0 mm), $<v> = 17.5$ cm/s, n=0.20. These represent a range of flow index values determined in these experiments. The curves show behavior intermittent between the limiting cases of Newtonian and plug flow. At n=0.85, the first appearance time (0.55) is closest to that of a Newtonian fluid, while at n=0.21 the first appearance time (0.68) is closest to plug flow. In addition, the time $t/<t>$ at which F=0.99 decreases as n decreases. In other words, the increasing pseudoplastic nature improves the uniformity of the history during pipe flow.

CONCLUSIONS

In summary, the information obtained by MRI for these systems is useful for understanding the flow of fluid/particulate mixtures at particle loadings that are relevant to aseptic processing. Furthermore, due to the opaque nature of these fluids, MRI is the only way to get this information. In these fluids, velocity profiles are increasingly blunted as (a) flow rate increases, (b) particle loading increases, and (c) particle size increases. The RTD is a function of the flow behavior index n that characterizes the rheological behavior in pipe flow. As the velocity profile becomes more blunt, n decreases and the fluid/particulate mixture is subjected to a more uniform flow history.

Strictly speaking, n is a true rheological parameter for only homogeneous fluids (no particles) in steady laminar flow. However, the flow behavior index allows us to describe the apparent rheological behavior of the fluid/particulate mixtures under the specified flow condition. This approach to modeling allows a straight-forward comparison of velocity profiles and residence time distributions (RTD) as a function of flow rate, particle loading, and particle size.

ACKNOWLEDGMENTS

This research was funded by the Center for Aseptic Processing and Packaging Studies (CAPPS).

REFERENCES

BUCHNER, N. 1993. Aseptic processing and packaging of food particulates. In *Aseptic Processing and Packaging of Particulate Foods*. (E.M.A. Willhoft, ed.) pp. 1–22, Blackie Academic and Professional, London.

CALLAGHAN, P.T. 1991. *Principles of Nuclear Magnetic Resonance Microscopy*. Oxford University Press, New York.

CAPRIHAN, A. and FUKUSHIMA, E. 1990. Flow measurements by NMR. Physics Reports. *198* (4), 195–235.

CARR, H.Y. and PURCELL, E.M. 1954. Effects of diffusion on free precession in nuclear magnetic resonance experiments. Physical Review *94*(3), 630–638.

FREGERT, J. and TRAGARDH, C. 1995. Solid-liquid flow in a horizontal pipe. *Proceedings of the International Symposium on Advances in Aseptic Processing and Packaging Technologies*, Copenhagen, Denmark.

HAHN, E.L. 1950. Spin echoes. Physical Review *80*(4), 580–594.

HONG, C.W., PAN, B.S., TOLEDO, R.T. and CHIOU, K.M. 1991. Measurement of residence time distribution of fluid and particles in turbulent flow. J. Food Science *56*(1), 255–259.

MIDDLEMAN, S. 1977. *Fundamentals of Polymer Processing*. pp. 301–303, McGraw-Hill Book Co., New York.

POPE, J.M. and YAO, S. 1993. Quantitative NMR imaging of flow. Conc. Mag. Res. *5*, 281–302.

SASTRY, S.K. 1989. Theoretical calculations for ensuring safe aseptic process design. *Activities Report of the R&D Associates*. Fall 1988 Meeting. U.S. Army Natick Research, Development & Engineering Center, Natick, MA.

SIMUNOVIC, J., SWARTZEL, K., FARKAS, B. and ADAMS, J. 1995. Particle residence time measurement of single and multiple solid phase particulate products in clear aseptic holding tube segments. *Proceedings of the International Symposium on Advances in Aseptic Processing and Packaging Technologies*, Copenhagen, Denmark.

SINGH, R.K. and LEE, J.H. 1992. Residence time distributions of foods with/without particulates in aseptic processing systems. In *Advances in Aseptic Processing Technologies* (R.K. Singh and P.E. Nelson, eds.) pp. 7–62, Elsevier Applied Science, London.

STEFFE, J.F. 1992. *Rheological Methods in Food Process Engineering*. p. 58, Freeman Press, East Lansing, MI.

STEJSKAL, E.O. 1965. Use of spin echoes in a pulsed magnetic field gradient to study anisotropic, restricted diffusion and flow. J. Chem. Phys. *43*, 3597–3603.

STEPISNIK, J. 1985. Measuring and imaging of flow by NMR. Prog. NMR Spect. *17*, 187–209.

TUCKER, G.S. and WITHERS, P.M. 1994. Determination of residence time distribution of nonsettling food particles in viscous food carrier fluids using Hall effect sensors. J. Food Process Engineering *17*, 401–422.

YANG, B.B. and SWARTZEL, K.R. 1992. Particle residence time distributions in two-phase flow in straight round conduit. J. Food Science *57*(2), 497–502.